ELSEVIER

PII: S0032-3861(97)00020-7

Polymer Vol. 38 No. 20, pp. 5211–5216, 1997

0032-3861/97/$17.00+0.00

Crosslinkings of polyacrylonitrile using NCO terminated urethanes

Young Se Oh
Research and Development Center, Hanil Synthetic Fiber Co., Masan 630-791, Korea

and Byung Kyu Kim*
Department of Polymer Science and Engineering, Pusan National University, Pusan 609-735, Korea
(Received 23 July 1996; revised 17 September 1996)

High nitrile terpolymers comprised of acrylonitrile (92 wt%), methyl acrylate (4 wt%), and hydroxylethyl methacrylate (4 wt%) (PAN) were synthesized and crosslinked using hexamethylene diisocyanate (HDI) terminated urethane prepolymer prepared from different molecular weights of poly(tetramethylene adipate) glycol (PTAd). The effects of urethane crosslinking and crosslinker length are studied. The degree of swell and soluble fraction of PAN increased dramatically and density decreased with crosslinker length. Wide angle X-ray diffraction showed an increase in the lateral repeat distance of hexagonal lattice as well as the crystalline size. The tan δ peak temperature of PAN decreased by crosslinking, however, the rubbery state extended with higher temperature, with the modulus (G_N^0) increasing as the crosslinker shortened. The undrawn crosslinked PAN showed ductile fracture with pronounced yielding and necking, whereas the undrawn linear PAN showed brittle fracture. The drawn linear PAN sample split into fibrils at the fracture tip, whereas the crosslinked PAN showed smooth fracture surfaces. © 1997 Elsevier Science Ltd.

(Keywords: polyacrylonitrile; NCO terminated urethane)

INTRODUCTION

High strength flexible-chain polymers are mainly manufactured with the help of orientational drawing. Many authors have published numerous experimental results on both the structural transformations and changes in the mechanical properties upon orientation[1–3]. It has been shown that the tensile strength and deformation modulus grow significantly as the draw ratio increases[1,4,5]. Many experimental methods to increase the draw ratio, including steam drawing, gel drawing, and zone drawing have been reported. However, the strengths of fibres and films prepared by these methods were considerably lower than the theoretical ones[6,7]. Many investigators are therefore interested in finding new ways to increase further the polymer strength in the production of fibres and films from synthetic materials. However, there are difficulties associated first of all with the fact that drawing ceases after a definite draw ratio is reached. In the case of polyacrylonitrile (PAN) protofibre spun through solution, the maximum draw ratio at failure is about 12–15 times the original protofibre in 100°C water, the value increases a little in pressurized steam. A number of papers[8–10] discuss some mechanisms for the orientational drawing process, but we believe that this problem for PAN requires a deeper consideration.

We have carried out structural modification of fibre-forming PAN to improve the drawability through the crosslinking reaction with diisocyanate (NCO) terminated urethanes.

* To whom correspondence should be addressed

EXPERIMENTAL

Preparation of PAN

Polymerization of high nitrile terpolymer (hereafter called PAN) was carried out in *N,N*-dimethyl formamide (DMF). Commercial grades of starting materials (dried DMF 400 g), acrylonitrile (AN) (92 g), methyl acrylate (MA) (4 g), hydroxylethyl methacrylate (HEMA) (4 g), and azobis-iso-butyronitrile (AIBN) (0.2 g) were charged into a four-necked flask equipped with a stirrer. After removing the oxygen by bubbling with nitrogen, polymerization proceeded with agitation at 70°C for 16 h. Once the polymerization was complete, the polymer solution was diluted with DMF (400 ml) and precipitated into methanol and washed 3 times with fresh water. The washed polymer was dried under vacuum at 50°C for 72 h. The intrinsic viscosity [η] and hydroxyl value of the prepared PAN were, respectively, 1.32 dl g^{-1} (DMF at 35°C) and 14.0, estimated by the AOAC 28.020 method[11].

Preparation of NCO-terminated polyurethane prepolymer[12–15]

Basic formulation is given in *Table 1*. One equivalent of poly(tetramethylene adipate) glycol (PTAd) of three different molecular weights was charged into a four-neck flask, equipped with a high-torque mechanical stirrer, thermometer, nitrogen inlet, and reflux condenser. After heating to 85°C, two equivalents of hexamethylene diisocyanate (HDI) were slowly added with stirring. Urethane forming reactions were carried out until the theoretical isocyanate value was reached, the value determined by the di(n-butyl)amine back titration

Table 1 Samples and component of crosslinker

Sample	Crosslinker	
	Amount (wt%)	Composition
PAN	—	—
PAN1	1.89	HDI
PAN2	5.17	HDI-PTAd(600)-HDI
PAN3	7.63	HDI-PTAd(1000)-HDI
PAN4	13.32	HDI-PTAd(2000)-HDI

HDI, Hexamethylene diisocyanate; PTAd, polytetramethylene adipate glycol; ( ), weight average molecular weight of PTAd

method[16]. It generally took about 2 h. The NCO-terminated PU prepolymer was then cooled at 0°C with dried nitrogen, and used as the crosslinker for the preparation of networked PAN films.

Preparation of PAN networked films

PAN with hydroxyl side chains was dissolved in dried DMF. This PAN-DMF solution (15 wt%) and diisocyanate (NCO-terminated urethane prepolymer) were mixed at 0°C until the PU prepolymer was completely dissolved. 0.01 wt% dibutyltin dilaurate (T-12) was carefully added, and air entrapped during mixing was removed by applying a vacuum. This mixture was poured into a stainless steel dish (110 mm o.d., 100 mm i.d., 2 mm height), which was placed in an oven at 85°C with exchanged dry air for 8 h, and then in a 40°C vacuum oven for another 72 h. Networked PAN film was peeled off from the dish and given three 1 h extractions in refluxing methanol (approximately 1 : 1000 weight ratio of film to methanol) to remove unreacted crosslinker. The weight loss of networked PAN film after extraction was less than 0.01 wt%. In the above crosslinking reaction, the amount of crosslinker was matched with a half equivalent of HEMA unit per PAN. Experimental details and types of crosslinker are also shown in *Table 1*.

Measurements of equilibrium swell and weight loss fraction

The networked PAN films of about 20 × 30 × 0.1 mm in size were swollen in DMF at room temperature for several days until the equilibrium state was reached. After weighing the swollen samples, the material was dried again in a vacuum oven at 50°C for 3 days and reweighed. The degree of swell and soluble fraction were calculated as follows:

$$\text{swelling}(\%) = [(W_s - W_2)/W_2] \times 100 \quad (1)$$

$$\text{solubles}(\%) = [(W_1 - W_2)/W_1] \times 100 \quad (2)$$

where W_1 is the dried weight of the film before swelling, W_2 is the dried weight after swelling, and W_s is the weight of DMF-swollen networked PAN film.

Density measurements

Density was measured using a density gradient column with tetrachloromethane/heptane as the medium. All measurements were made at 25°C. The experimental error was $\pm 0.004\,\text{g cm}^{-3}$, and the average of three measurements for each sample was taken.

X-ray diffraction measurement

X-ray diffractograms of the networked PAN film samples were obtained using a Rigaku XG X-ray generator at 35 kV, 20 mA. The scattered X-ray in WAXD mode was monochromatized to CuK_α with a graphite monochromator, and counted with a Rigaku Denki scintillation counter at intervals of 0.05° scattering angle using a Rigaku Rint 2000 goniometer. The apparent crystallite size was estimated from the profile of the (100) difraction. Having been corrected for the air scattering, the half-width of the profile Δw_p was estimated. The correction for the instrumental broadening was made using equation (3), where Δw_a is the half-width of the diffraction profile at $2\theta = 28.5°$ of powdered silicon used as a standard material.

$$\Delta w^2 = \Delta w_p^2 - \Delta w_a^2 \quad (3)$$

The apparent crystallite size t (Å) was calculated from the estimated intrinsic broadness Δw, using Scherrer's equation:

$$t = \frac{k\lambda}{\Delta w \cos\theta} \quad (4)$$

where k is a constant (0.94), θ is the Bragg angle, and Δw is expressed in radians.

Dynamic and tensile property measurements

Dynamic mechanical properties of networked PAN films were measured using a Rheovibron (Orientec DDV-01FP) at 11 Hz, from 25° to 250°C. Tensile properties of undrawn and drawn films were measured at room temperature following the standard procedure in ASTM D412 with type C specimens using Tensilon (Shimadzu, Autograph S-100), operated at $50\,\text{mm m}^{-1}$. The draw ratio [20 mm (l) × 40 mm (w) × 0.1 mm (h)] at failure (DR_{max}) was estimated using a mechanical drawing machine which was operated at 100°C in water.

SEM observation

The fractured samples were prepared by stretching the films to 100% on a Tensilon at room temperature. The fractured samples were slightly sputtered with gold and examined under scanning electron microscopy (JSM 6400).

RESULTS AND DISCUSSION

Swell and density

The degree of swell, soluble fraction, and density of the film are shown in *Table 2*. With increasing crosslinker length, the degree of swell and soluble fraction increase dramatically, whereas the density decreases slightly. Crosslinking occurs between the two OH groups of different chains and one NCO-terminated urethane crosslinker. Reaction can also occur between the two OH groups of the same chain and urethane crosslinker. However, this type of self-crosslinking does not contribute to the elasticity, solvent and thermal

Table 2 Degree of swell, soluble fraction, and density of the samples

Sample	Swelling (wt%)	Soluble fraction (wt%)	Density (g cm^{-3})
PAN	—	100.0	1.176
PAN1	325	1.54	1.173
PAN2	1412	13.94	1.169
PAN3	2916	21.82	1.164
PAN4	2538	30.54	1.148

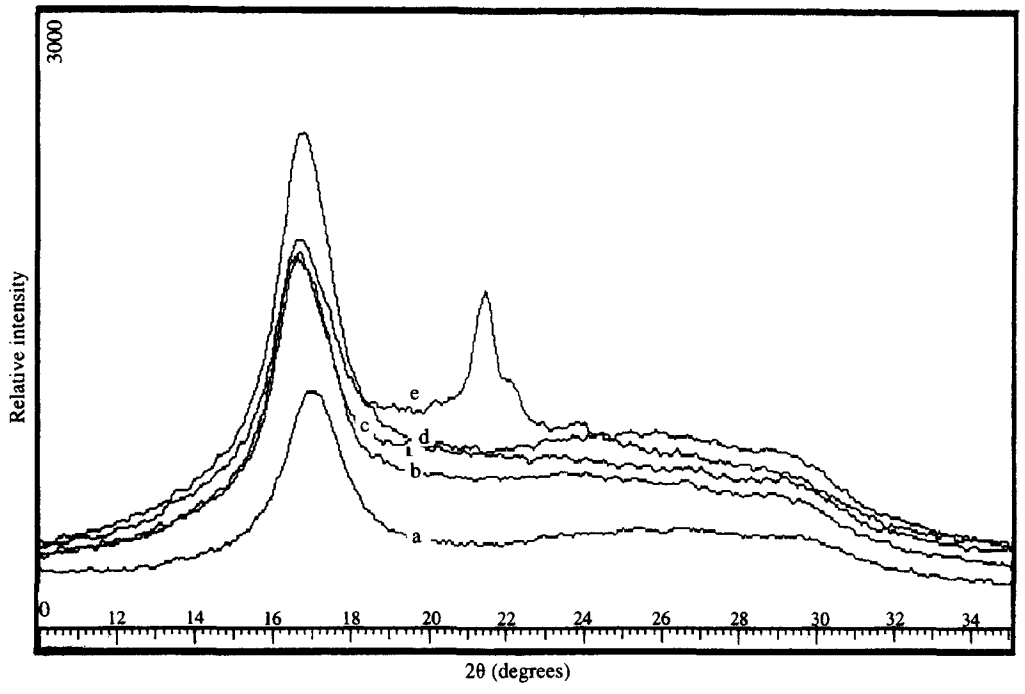

Figure 1 Wide angle X-ray diffractograms for the linear and crosslinked PAN films: (a) PAN, (b) PAN1, (c) PAN2, (d) PAN3, (e) PAN4

Table 3 Parameters from wide angle X-ray diffraction of PAN films

			Apparent crystallite size		Degree of crystallinity	
Sample	2θ	Bragg spacing (Å)	Half width (Δw)	t (Å)	CC[a]	CC[b]
PAN	17.00	5.23	1.735	48.9	0.641	0.420
PAN1	16.70	5.30	1.703	49.9	0.603	0.419
PAN2	16.60	5.325	1.728	49.1	0.515	0.369
PAN3	16.55	5.357	1.682	50.6	0.398	0.307
PAN4	16.45	5.373	1.610	53.1	0.419	0.311
	21.00	4.230	0.488	167.53		

[a] The coefficient of crystallinity determined by the Hinrichsen method
[b] The crystallinity index determined by the Bell and Dumbleton method

resistance of the PAN polymers. With the increase in crosslinker length, crosslink density is decreased leading to increased swell and decreased density. On the other hand, the soluble fraction increase with increasing crosslinker length is mainly due to the increased self-crosslinks. This reaction becomes possible only with a long crosslinker since the pendant OH groups are randomly and rarely distributed along the main chain PAN. The density of networked PAN decreases with the increase of crosslinker molecular weight. Density changes are related to the level of crystallinity or packing of crystallite, in addition to the crosslinking density. With the increase of crosslinker size, the crystallinity of the PAN chain decreases due to the incorporation of crosslinking segment into the crystallite. This result agrees well with the X-ray diffractograms below.

X-ray diffraction

Wide-angle X-ray diffractograms showing the radial scans of the intensity vs angle of diffraction (2θ) for PAN and networked PAN films are shown in *Figure 1*. Generally, the diffractogram of PAN shows a moderately sharp intense diffraction at $2\theta = 16.5°$ (peak 1) and a less intense diffraction at $2\theta = 29.5°$ (peak 2) interspread by a broad diffuse scattering maximum situated around $2\theta = 25°–27°$. Peak 2, however, is superimposed on the diffuse scattering maximum and completely absent in some cases[17–19]. The sharp intense diffraction (peak 1) corresponds to a lateral repeat distance or Bragg spacing and has been represented as the (100) diffraction of the hexagonal lattice[20]. The reflection at $2\theta = 29.5°$ (peak 2) confirms the second-order diffraction of peak 1[21]. As shown in *Figure 1*, the position of peak 1 diffraction on the 2θ axis moved to a lower angle for networked PAN film samples. This implies that the Bragg spacing increases. Another peak at $2\theta = 21.0°$ in the PAN4 sample seems to come from the PTAd unit. Structural parameters for those samples evaluated from the X-ray diffraction data are shown in *Table 3*. The d-spacing of peak 1 for linear PAN is 5.23 Å ($2\theta = 17.0°$) corresponding to the (100) diffraction of the hexagonal lattice. For the networked PAN samples, d-spacings and sizes of apparent crystallite are increased, while the degree of crystallinity is decreased with increasing crosslinker molecular weight. The increase in Bragg spacing indicated some change in the crystalline lattice. Such an effect could be due to the reduced perfection at the crystallite boundaries produced by crosslinkers, reducing the degree of crystallinity.

Dynamic mechanical properties

The storage modulus (E') and tan δ of the samples are shown in *Figures 2* and *3*, respectively. For linear PAN, there is a large decrease in E' at the glass transition temperature of PAN which showed up as a relatively sharp loss peak around 100°C. A drop in E' and rise in tan δ above 200°C is associated with the thermal decomposition of linear PAN. Upon crosslinking the PANs, the initial relaxation temperature is slightly decreased below the linear PAN, however, the rubbery plateau extends to much higher temperature due to the increased thermal resistance of the PAN. Notably the magnitude of plateau modulus (G_N^o) decreases with increasing crosslinker length. For ideal rubbers where entropy change upon extension governs the elasticity, the plateau modulus is given by

$$G_N^o = \frac{\rho RT}{M_c} \quad (5)$$

where ρ, R, T, and M_c are the density, ideal gas constant, absolute temperature, and molecular weight between crosslinks, respectively. In our experiments, the same equivalents of crosslinkers were used, so the main chain molecular weight between crosslinks (M_c) should be the same. We, therefore, can imagine that the effect of increased crosslinker length on the plateau modulus is similar to the increased main chain length between the crosslinks. In vulcanization of rubber, crosslinker lengths are controlled by the relative amount of sulfur and accelerator. With more accelerator and less sulfur, short crosslinks are obtained, resulting in an increased modulus and thermal stability, and decreased elasticity.

Tensile properties

The plots of specific stress vs strain for undrawn and drawn samples are shown in *Figures 4* and *5*, and the important values are summarized in *Tables 4* and *5*. The undrawn, linear PAN films are deformed in a very brittle manner, and the undrawn networked PAN films show ductile deformation with pronounced yielding and necking (Fig. 4). Yielding is more pronounced with shorter crosslinkers. Regardless of drawing, yield strength decreases with increasing molecular weight of crosslinker. This result comes from the level of crystallinity. In addition, yielding is governed by some processes involving deformation or transformation of part or all of the crystalline regions. When a small force is applied to the sample, i.e. within the elastic region,

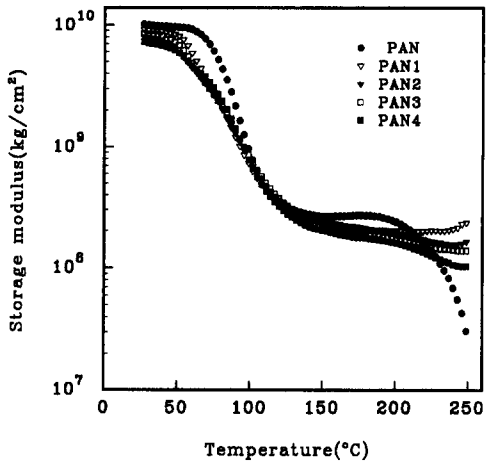

Figure 2 Storage modulus vs temperature for the linear and crosslinked PAN films

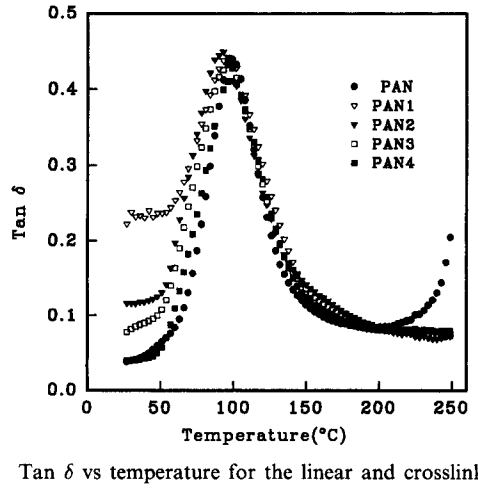

Figure 3 Tan δ vs temperature for the linear and crosslinked PAN films

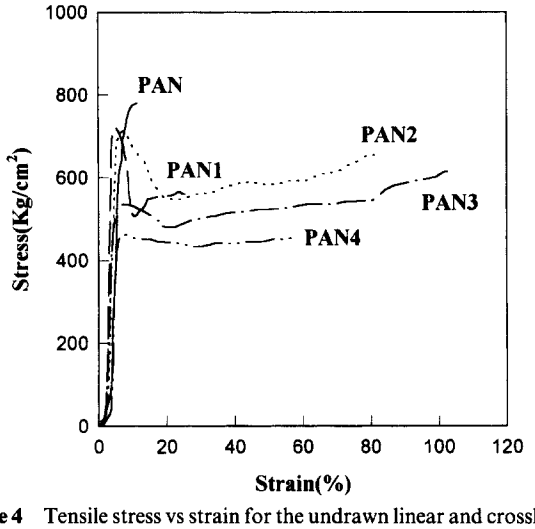

Figure 4 Tensile stress vs strain for the undrawn linear and crosslinked PAN films

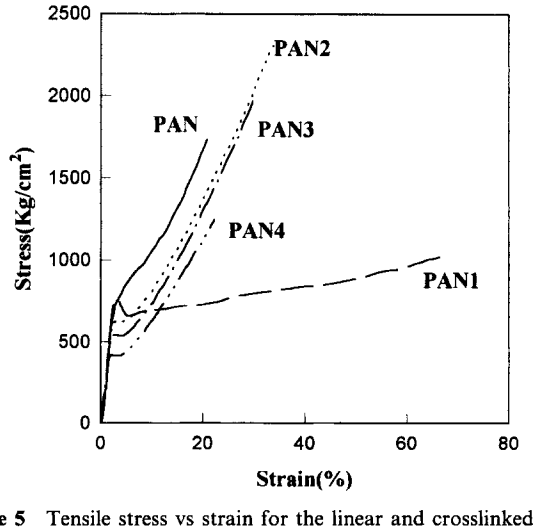

Figure 5 Tensile stress vs strain for the linear and crosslinked PAN films drawn at failure

extension will occur for two reasons: (i) a slight stretching of the chain molecules themselves, and (ii) a straightening of the molecules in the non-crystalline regions, resulting in the straining of the crosslinkings between them. When the applied force becomes large, some of the highly strained crosslinking in the crystalline boundary region will partially melt or break because they cannot support the force applied in them. Consequently, at yield, extension becomes much easier. On the other hand, the DR_{max} of PAN film is 25 times, but networked PAN films can be drawn over 50 times depending on the crosslinker type. What is the reason for a relatively high drawability of networked PAN films? It is known that in plastic deformation of a microfibrillar structure, different modes leading to an increase in the macroscopic

Table 4 Tensile properties of undrawn samples

Sample	Tensile strength ($kg\,cm^{-2}$)	Yield strength ($kg\,cm^{-2}$)	Elongation (%)
PAN	763	745	16
PAN1	552	712	22
PAN2	662	705	82
PAN3	614	521	103
PAN4	472	476	61

Table 5 Tensile properties of drawn samples

Sample	DR_{max}	Tensile strength ($kg\,cm^{-2}$)	Yield strength ($kg\,cm^{-2}$)	Elongation (%)
PAN	25	1725	783	17
PAN1	7	896	774	73
PAN2	38	2353	633	33
PAN3	52	1942	589	29
PAN4	47	1235	409	21

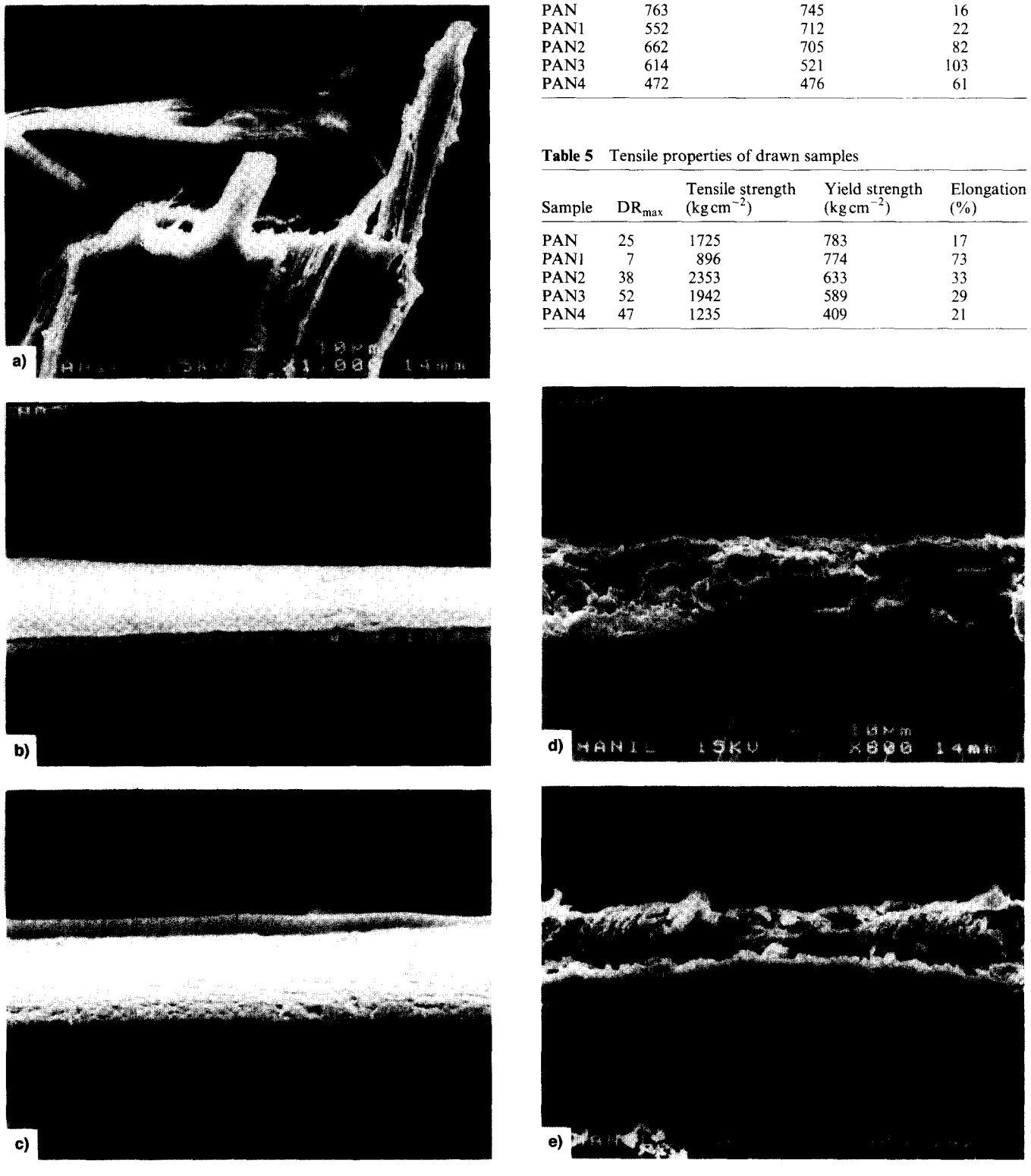

Figure 6 SEM micrographs of fractured cross section for the drawn linear and crosslinked PAN films: (a) PAN, (b) PAN1, (c) PAN2, (d) PAN3, (e) PAN4

dimensions of sample in the draw direction can occur. These modes are a rotation of otherwise unaltered crystallites, a change in the chain orientation within the crystallites, and a separation of the crystallites due to extension of the amorphous interlayers between them[22–24], and the microfibrillar slip[25]. During drawing of films we have observed an increase of degree of order, *d*-spacing, and crystallite dimension measured by the reduction in the half-width of the equatorial reflection (100) (*Figure 1*). It may be inferred from this fact that none of the deformation modes mentioned above occurs during the orientational drawing of films, except the microfibrillar slip. A number of authors supposed that microfibrils can be connected with each other by so-called interfibrillar tie molecules[25,26]. In the case of networked PAN films, tie molecules are bonded with interfibrils. Obviously, the number of such molecules, their conformation, and distribution by their lengths can significantly influence the slip. It seems that the shorter crosslinkers play a role in restraining the slip of PAN microfibrils like PAN1 film. However, the relatively low drawability of PAN4 film compared to PAN3 film seems to come from phase separation between microfibrils and large crosslinker moieties. In X-ray diffraction of PAN4 film, the peak ($2\theta = 21.0°$) corresponding to the PTAd unit was observed. In fact, it is observed that the transparency of networked PAN films decreased with an increase of molecular weight of the crosslinker. On the other hand, the main reason for the termination of the orientational drawing in polymers is a closer packing of microfibrils hindering a further axial displacement of microfibrils and leading to an increase in the orientational stress up to a critical value. The closest packing of microfibrils is observed for non-cross-linked PAN sample by the X-ray diffraction and density data.

Tensile strength for undrawn samples is governed by the crystallinity level of the samples, as expected, whereas for drawn samples tensile strength is mainly dominated by orientation and crystallinity (*Table 5*). The maximum improvement of tensile strength in response to orientation is achieved with networked PAN2, not with PAN3 or PAN4. This implies that the relatively longer tie molecules introduced by a foreign crosslinker is not a factor for tensile strength improvement, although it is a good factor for orientation. It is presumed that the longer tie molecules of the foreign crosslinker should form a self-domain in the PAN matrix and, consequently, a decrease in tensile strength is expected due to low crystallinity.

Fractography

Figure 6 shows scanning electron micrographs of the fractured surfaces of drawn PAN samples. The drawn samples were fractured using the tensile tester at room temperature. The fractured tip of drawn PAN sample split into fibrils (*Figure 6a*). However, fibrillar structures are not found in the fractured tips of drawn networked PAN samples, and smooth surfaces are shown with variation of the size of crosslinkers (*Figures 6b–e*). It is supposed that the splitting of fibrils at the tip arises from the applied tensile stress when fibrils are well developed along the axial direction. In the case of networked PAN samples, a smooth surface in fractured section is a result of the formation of a bridge between intermicrofibrils preventing fibril splitting. Thus, the smooth-faced surface was enhanced by increasing the degree of crosslinking. This means crosslinking segments exist at the boundary of crystallites, providing a less perfect crystallinity.

REFERENCES

1. Savitskii, A. V., Levin, B. Y. and Demitcheva, V. P., *Vysokomol. Soedin.*, 1973, **A14** (6), 1286.
2. Marikhin, V. A. and Myasnikova, L. P., *J. Polym. Sci., Polym. Symp.*, 1977, **58**, 97.
3. Geil, P. H., *Polymer Single Crystals*. Interscience, New York, 1964.
4. Capaccio, G., Chapman, T. J. and Ward, I. M., *Polymer*, 1975, **16**, 469.
5. Barham, P. J. and Keller, A., *J. Mater. Sci.*, 1976, **11**, 27.
6. Perepelkin, K. B., *Angew. Makromol. Chem.*, 1972, **22**, 181.
7. Sakurada, I. and Kaji, K., *J. Polym. Sci., C*, 1970, **31**, 57.
8. Sadler, D. M. and Barham, P. J., *Polymer*, 1990, **31**, 36.
9. Sadler, D. M. and Barham, P. J., *Polymer*, 1990, **31**, 46.
10. David, D. J. and Staley, H. B., *Analytical Chemistry of Polyurethanes*, High Polymer Series, XVI, Part III. Wiley-Intersciences, New York, 1969.
11. Wu, W., Wignall, G. D. and Mandelkern, L., *Polymer*, 1990, **33**, 4137.
12. Kim, B. K. and Lee, J. C., *Polymer*, 1996, **37** (3), 469.
13. Lee, Y. M., Lee, J. C. and Kim, B. K., *Polymer*, 1994, **35** (5), 1095.
14. Lee, K. H. and Kim, B. K., *Polymer*, 1996, **37** (11), 2251.
15. Kim, B. K., Lee, S. Y. and Xu, M., *Polymer*, 1996, **37**(26), 5781.
16. Hinrichsen, G. and Orth, H., *J. Polym. Sci. B.*, 1971, **9**, 529.
17. Bell, J. P. and Dumbleton, J. P., *Text. Res. J.*, 1971, **41**, 196.
18. Gupta, A. K. and Singhal, R. P., *J. Polym. Sci., Polym. Phys. Ed.*, 1987, **21**, 2243.
19. Sotton, M., Arniaud, A. M. and Rabourdin, C., *Bull. Sci. Inst. Text. Fr.*, 1978, **7**, 265.
20. Imai, Y., Mianmi, S., Yoshihara, T., Joh, Y. and Saito, H., *J. Polym. Sci., Polym. Lett., Ed.*, 1970, **8**, 281.
21. Cowking, A., Rider, J. G., Hay, I. L. and Keller, A., *J. Mater. Sci.*, 1968, **3**, 646.
22. Keller, A. and Pope, D. P., *J. Mater. Sci.*, 1971, **6**, 453.
23. Slitsker, A. I., Aanphirova, T. P., Yastrebinskii, A. I. and Kuksenko, V. S., *J. Polym. Sci.*, 1973, **C42**, 847.
24. Hearle, J. W. S., *J. Polym. Sci.*, 1958, **28**, 432.
25. Petelrin, A., *Colloid Polym. Sci.*, 1975, **253**, 809.
26. Konatsu, T., *J. Mater. Sci.*, 1993, **28**, 3035.